

Ergodicity Test of the Eddy Correlation Method

Jinbei CHEN^{1,2} Yinqiao HU^{2,*} Ye YU^{1,2} Shihua LÜ¹

1 Key Laboratory of Land Surface Processes and Climate Change in Cold and Arid Regions; Cold and Arid Regions Environment and Engineering Institute, Chinese Academy of Sciences, Lanzhou 730000, P R China.

2 Pingliang Land Surface Process & Severe Weather Research Station, Chinese Academy of Science, Pingliang 744015, P R China.

E-mail: chenjinbei@lzb.ac.cn

* Corresponding author: hyq@ns.lzb.ac.cn

Abstract

The ergodic hypothesis is a basic hypothesis in atmospheric turbulent experiment. The ergodic theorem of the stationary random processes is introduced first into the turbulence in atmospheric surface layer (ASL) to analyze and verify the ergodicity of atmospheric turbulence measured by the eddy covariance system with two sets of field observational data of the ASL. The results show that eddies of atmospheric turbulence, of which the scale is smaller than the scale of atmospheric boundary layer (ABL), i.e. the spatial scale is less than 1,000 m and temporal scale is shorter than 10 min, can effectively satisfy the ergodic theorems. Therefore, the finite time average can be used to substitute for the ensemble average of atmospheric turbulence. Whereas, eddies are larger than ABL's scale, cannot satisfy the mean ergodic theorem. Consequently, when the finite time average is used to substitute for the ensemble average, the eddy correction method would occur a large error rate due to the losing low frequency information of the larger eddies. The multi-station observation is compared with the single-station, and then the scope that satisfies the ergodic theorems is expanded from the smaller scale about 1000 m of ABL's scale to about 2000 m, even it exceeds ABL's scale. Therefore, the calculation of average, variance and fluxes of the turbulence can effectively satisfy the ergodic assumption, and the results are more approximate to the actual values. Regardless of vertical velocity or temperature, the variance of eddies in different scales can more efficiently follow Monin-Obukhov Similarity Theory (MOST), if the ergodic theorem can be satisfied; or else it deviates from MOST. The ergodicity exploration of the atmospheric turbulence is doubtlessly helpful to understanding the issues in atmospheric turbulent observation, and provides a theoretical basis for overcoming related difficulties.

35 **Keywords:** Ergodic hypothesis; eddy-correlation method; Monin-Obukhov similarity
36 theory (MOST); atmospheric surface layer (ASL); high-pass filtering

37

38 **1 Introduction**

39 The basic principle of average of the turbulence measurement is the ensemble average
40 of space, time and state. However, it is impossible that an actual turbulence
41 measurement with numerous observational instruments in space for enough time to
42 obtain all states of turbulent eddies to achieve the goal of ensemble average.
43 Therefore, based on the ergodic hypothesis, the time average at one spatial point,
44 which is long enough for observation, is used to substitute for the ensemble average
45 for temporally steady and spatially homogeneous surface (Stull 1988; Wyngaard 2010;
46 Aubinet 2012). The ergodic hypothesis is a basic assumption in atmospheric turbulent
47 experiment of the atmospheric boundary layer (ABL) and atmospheric surface layer
48 (ASL). The stationarity, homogeneity, and ergodicity are routinely used to link the
49 ensemble statistics (mean and higher-order moments) of field observational
50 experiments in the ABL. Many authors habitually refer to the ergodicity assumption,
51 as some descriptions such as “when satisfying ergodic hypothesis,” or
52 “something indicates that ergodic hypothesis is satisfied”. Though the success of
53 Monin-Obukhov Similarity Theory (MOST) for unstable and near-neutral conditions
54 is just an evidence of ergodic hypothesis validity in the ASL, however it is only a
55 necessary condition for ergodicity in the ASL experiments, does not proves ergodicity
56 (Katul et al., 2004). MOST success is under the conditions of stationary and
57 homogeneous surface. It implies that the stationarity and homogeneity are the
58 important conditions of ASL ergodicity. Therefore, many ABL’s experiments focus
59 on seeking ideal homogeneous surface as much as possible. And some test procedures
60 of availability are widely applied to establish stationarity (Foken and Wichura 1996;
61 Vickers and Mahrt 1997). Katul et al. (2004) qualitatively analyzed the ergodicity
62 problems in regarding atmospheric turbulence, and believed that it is common for the
63 neutral and unstable stratification in ASL to reach ergodicity, while it is difficult to
64 reach ergodicity for the stable layer. Eichinger et al. (2001) indicate that LIDAR
65 (Light Detection and Ranging) technique opens up new possibilities for atmospheric
66 measurements and analysis by providing spatial and temporal atmospheric
67 information with simultaneous high-resolution. The stationarity and ergodicity can be

68 tested for such ensembles of experiments. Recent advances in LIDAR measurements
69 offers a promising first step for direct evaluation of such hypotheses for ASL flows
70 (Higgins et al., 2013). Higgins et al. (2013) applied LIDAR of water vapor
71 concentration to investigate the ergodic hypothesis of atmospheric turbulence for the
72 first time. It is clear all the same that there is a need to reevaluate turbulence
73 measurement technology, to test the ergodicity of atmospheric turbulence
74 quantitatively by means of observation experiments.

75 The ergodic hypothesis was first proposed by Boltzmann (Boltzmann 1871; Uffink
76 2004) in his study of the ensemble theory of statistical dynamics. He argued that a
77 trajectory traverses *all* points on the energy hypersurface after a certain amount of
78 time. At the beginning of 20th century, Ehrenfest' couple proposed the quasi-ergodic
79 hypothesis and changed the term "traverses *all* points" in aforesaid ergodic hypothesis
80 to "passes arbitrarily close to every point". The basic points of ergodic hypothesis or
81 quasi-ergodic hypothesis recognize that the macroscopic property of system in the
82 equilibrium state is the average of microcosmic quantity in a certain amount of time.
83 Nevertheless, the ergodic hypothesis or quasi-ergodic hypothesis were never proven
84 theoretically. The proof of ergodic hypothesis in physics aroused the interest of
85 mathematicians. The famous mathematician, Neumann et al. (1932) first theoretically
86 proved the ergodic theorem in topological space (Birkhoff 1931, Krengel 1985).
87 Afterward, a banaisic ergodic theorem of stationary random processes was proved to
88 provide the necessary and sufficient conditions for the ergodicity of stationary random
89 processes. Mattingly (2003) reviewed research progress of the ergodicity of random
90 Navier-Stokes equations, and Galanti (Galanti et al. 2004, Lennaert et al. 2006) solved
91 the random Navier-Stokes equation by numerical simulation to prove that the
92 turbulence which is temporally steady and spatially homogeneous is ergodic.
93 However, Galanti (2004) also indicated that such partially turbulent flows acting as
94 mixed layer, wake flow, jet flow, flow around the boundary layer may be non-ergodic
95 turbulence.

96 Obviously, the advances of research on the ergodicity in the mathematics and
97 physics have precedence far over the atmospheric science. We try firstly to introduce
98 the ergodic theorem of stationary random processes to atmospheric turbulence in ASL
99 in this paper. And that the ergodicity of different scale eddies of atmospheric
100 turbulence is directly analyzed and verified quantitatively on the basis of the field

101 observational data measured by the eddy covariance system.

102 **2 Theories and methods**

103 **2.1 Ergodic theorems of stationary random processes**

104 The stationary random processes are the processes which will not vary with time, i.e.,
105 for observed quantity A , its function of spatial x_i and temporal t_i satisfies the following
106 condition:

$$107 A(x_1, x_2, \dots, x_n; t_1, t_2, \dots, t_n) = A(x_1, x_2, \dots, x_n; t_1 + \tau, t_2 + \tau, \dots, t_n + \tau), \quad (1)$$

108 where τ is a time period, defined as the relaxation time.

109 The mean μ_A of random variable A and autocorrelation function $R_A(\tau)$ are
110 respectively defined as following:

$$111 \mu_A = \lim_{T \rightarrow +\infty} \frac{1}{T} \int_0^T A(t) dt, \quad (2)$$

$$112 R_A(\tau) = \lim_{T \rightarrow +\infty} \frac{1}{T} \int_0^T A(t)A(t + \tau) dt. \quad (3)$$

113 The autocorrelation function $R_A(\tau)$ is a temporal second-order moment. In the case of
114 $\tau=0$, the autocorrelation function $R_A(\tau)$ is the variance of random variable. The
115 necessary and sufficient conditions that stationary random processes satisfy the mean
116 ergodicity are the mean ergodic function $Ero(A)$ to zero (Papoulis et al. 1991), as
117 shown below:

$$118 Ero(A) = \lim_{T \rightarrow \infty} \frac{1}{T} \int_0^{2T} \left(1 - \frac{\tau}{2T}\right) [R_A(\tau) - \mu_A^2] d\tau = 0. \quad (4)$$

119 The mean ergodic function $Ero(A)$ is a time integral of variation between the
120 autocorrelation function $R_A(\tau)$ of variable A and its mean square, μ_A^2 . If the mean
121 ergodic function $Ero(A)$ converges to zero, then the stationary random processes will
122 be ergodic. In other words, if the autocorrelation function $R_A(\tau)$ of variable A
123 converges to its mean square, μ_A^2 , the stationary random processes are mean ergodic.

124 The Eq. (4) is namely the mean ergodic theorem to be called as well as ergodic
125 theorem of the *weakly* stationary processes in mathematics. For discrete variables, Eq.
126 (4) can be rewritten as the following:

$$127 Ero(A) = \lim_{n \rightarrow \infty} \sum_{i=0}^n \left(1 - \frac{\tau_i}{n}\right) [R_A(\tau_i) - \mu_A^2] = 0. \quad (5)$$

128 The Eq. (5) is the mean ergodic theorem of discrete variable. Hence, Eqs. (4) and (5)

129 can be used as a criterion to judge the mean ergodicity.

130 The necessary and sufficient conditions that stationary random processes satisfy the
 131 autocorrelation ergodicity are the autocorrelation ergodic function $Er(A)$ to zero:

$$132 \quad Er(A) = \lim_{T \rightarrow \infty} \frac{1}{T} \int_0^{2T} \left(1 - \frac{\tau'}{2T}\right) [B(\tau') - |R_A(\tau)|^2] d\tau' = 0; \quad (6a)$$

$$133 \quad B(\tau') = E \left\{ A(t + \tau + \tau') A(t + \tau') [A(t + \tau) A(t)] \right\}. \quad (6b)$$

134 Where τ' is a differential variable for entire relaxation times, and that $B(\tau')$ is the
 135 temporal fourth-order moment of variable A . The autocorrelation ergodic function
 136 $Er(A)$ is a time integral of variation between the temporal fourth-order moment $B(\tau')$
 137 of variable A and its autocorrelation function square, $|R_A(\tau)|^2$. If the autocorrelation
 138 ergodic function $Er(A)$ converges to zero, then the stationary random processes will be
 139 of autocorrelation ergodicity, and thus the autocorrelation ergodicity means that the
 140 fourth-order moment of the variable of stationary random processes will converge to
 141 square of its autocorrelation function $R_A(\tau)$. The Eq. (6a) is namely the autocorrelation
 142 ergodic theorem to be called as well as the ergodic theorem of *strongly* stationary
 143 processes in the mathematics. The autocorrelation ergodic function of corresponding
 144 discrete variable can be determined as following:

$$145 \quad Er(A) = \lim_{n \rightarrow \infty} \sum_{i=0}^n \left(1 - \frac{\tau'_i}{n}\right) [B(\tau'_i) - |R_A(\tau_j)|^2] = 0, \quad (7a)$$

$$146 \quad B(\tau'_i) = E \left\{ \sum_{j=0}^n A(t + \tau_j + \tau'_i) A(t + \tau'_i) [A(t + \tau_j) A(t)] \right\}. \quad (7b)$$

147 The Eq. (7a) is the autocorrelation ergodic theorem of discrete variable. Hence, Eqs.
 148 (6a) and (7a) can also be used as a criterion to judge autocorrelation ergodicity.

149 The stationary random processes conform to the criterion, Eqs. (4) or (5), viz.
 150 satisfy the mean ergodic theorem, or are intituled as the mean ergodicity; The
 151 stationary random processes conform to Eqs. (6a) or (7a), viz. satisfy the
 152 autocorrelation ergodic theorem, or are intituled as the autocorrelation ergodicity. If
 153 the stationary random processes are only of mean ergodicity, then they are the strict
 154 ergodic or narrow ergodic. If the stationary random processes are of both the mean
 155 ergodicity and autocorrelation ergodicity, then they are the wide ergodic stationary
 156 random processes. It is thus clear that the ergodic random processes are stationary, but

157 the stationary processes may not be ergodic.

158 With respect to the random process theory, when the mean and high-order moment
159 function is calculated, a large amount of repeated observations of random processes
160 require to acquire the sample function $A_i(t)$. If the stationary random processes satisfy
161 the ergodic conditions, then the time average of a sample on the whole time shaft can
162 be used to substitute for the overall or ensemble average. Eqs. (4), (5), (6a) and (7a)
163 can be used as the criterion to judge whether or not satisfying the mean and
164 autocorrelation ergodicity. The ergodic random processes must be the stationary
165 random processes to be defined as Eq. (1), and thus are stationary in relaxation time τ .
166 If conditions such as Eqs (4) and (5) of the mean ergodicity are satisfied, then a time
167 average in finite relaxation time τ can be used to substitute for the infinite time
168 average to calculate mean Eq. (2) of the random variable; similarly, the finite time
169 average can be used for substitution to calculate the covariance or variance of random
170 variable, Eq. (3), if conditions such as Eqs. (6a) and (7a) of autocorrelation ergodicity
171 are satisfied. In a similar manner, the basic principle of average of atmospheric
172 turbulence measurement is the ensemble average of space, time and state, and it is
173 necessary to carry through mass observation for a long period of time in the whole
174 space. This is not only a costly observation, even is hardly feasible. If the turbulence
175 signals satisfy the ergodic conditions, then the time average in relaxation time τ by
176 multi-station observation, even single-station observation, can substitute for the
177 ensemble average. In fact, the precondition to estimate the turbulent characteristic
178 quantities and fluxes in ABL by the eddy correlation method is that the turbulence
179 satisfies the ergodic conditions. Therefore, conditions such as Eqs. (4), (5), (6a) and
180 (7a) will also be the criterion for testing authenticity of the results observed by the
181 eddy correlation method.

182 **2.2 Band-pass filtering**

183 In the spatial scale, the atmospheric turbulence from the dissipation range, inertial
184 sub-range to the energy range, and further the turbulent large eddy is extremely broad
185 (Stull 1988). Such spatial and temporal size of eddies include the isotropic 3-D eddy
186 structure of high frequency turbulence and orderly coherent structure of low
187 frequency turbulence (Li et al. 2002). The different scale eddies are also different in
188 terms of their spatial structure and physical properties, and even their transport
189 characteristics are not all the same. It is thus reasonable that the eddies with different

190 transport characteristics are separated, processed and studied by using different
 191 methods (Zuo et al. 2012). A major goal of our study is to understand what type of
 192 eddy in the scale can satisfy the ergodic conditions. The another goal is that the time
 193 averaging of signals measured by a single station determines accurately the turbulent
 194 characteristic quantities. In order to study the ergodicity of different scale eddies,
 195 Fourier transform is used as band-pass filtering to distinguish the different scale eddy.
 196 That is to say, we set the Fourier transform coefficients of the part of frequencies,
 197 which does not need, as zero, and then acquire the signals after filtering by means of
 198 Fourier inverse transformation. The specific formulae are shown below:

$$199 \quad F_A(n) = \frac{1}{N} \sum_{k=0}^{N-1} A(k) \cos\left(\frac{2\pi nk}{N}\right) - \frac{i}{N} \sum_{k=0}^{N-1} A(k) \sin\left(\frac{2\pi nk}{N}\right), \quad (8)$$

$$200 \quad A(k) = \sum_{n=a}^{N-1} F_A(n) \cos\left(\frac{2\pi nk}{N}\right) + i^2 \sum_{n=a}^{N-1} F_A(n) \sin\left(\frac{2\pi nk}{N}\right). \quad (9)$$

201 In Eqs. (8) and (9), $F_A(n)$ and $A(k)$ are respectively the Fourier transformation and
 202 Fourier inverse transformation including N data points from $k=0$ to $k=N-1$, and n is the
 203 cycle index of the observation time range. The high-pass filtering can cut off the low
 204 frequency signals of turbulence to obtain high frequency signals. The aliasing of half
 205 high frequency turbulence after the Fourier transformation is unavoidable. At the
 206 same time, the correction for high frequency response will compensate for the loss. In
 207 order to acquire purely high frequency signals in the filtering processes, we take the
 208 results of band-pass filtering from $n=j$ to $n=N-j$ as the high frequency signals. This is
 209 referred to as j time filtering in this paper. Finally, the ergodicity of different scale
 210 eddies is analyzed using Eqs. (4)-(7).

211 **2.3 MOS of turbulent variance**

212 The characteristics of the relations of Monin-Obukhov Similarity (MOS) of the
 213 variance for the different scale eddies are analyzed and compared to test the feasibility
 214 of MOS's relation for the ergodic and non-ergodic turbulence. The problems of eddy
 215 correlation method in the turbulence observation in ASL are further explored on the
 216 basis of the study on the ergodicity and MOS's relations of the variance of different
 217 scale eddies in order to provide an experimental basis for utilizing MOST and
 218 developing the turbulence theory of ABL with complex underlying surfaces.

219 The MOS's relations of turbulent variance can be regarded as an effective
 220 instrumentality to verify whether or not the turbulent flow field is steady and

221 homogeneous (Foken et al. 2004). Under ideal conditions, the local MOS's relations
 222 of the variance of wind velocity, temperature and other factors can be expressed as
 223 following:

$$224 \quad \sigma_i/u_* = \phi_i(z/L), \quad (i = u, v, w), \quad (10)$$

$$225 \quad \sigma_s/|s_*| = \phi_s(z/L), \quad (s = \theta, q). \quad (11)$$

226 where σ is the turbulent variance; corner mark i is the wind velocity u , v or w ; s stands
 227 for scalar, such as potential temperature θ and humidity q ; u_* is the friction velocity
 228 and defined as $u_* = (\overline{u'w'^2} + \overline{v'w'^2})^{1/4}$; s_* is the turbulent characteristic quantity of
 229 the related scalar and defined as $s_* = -\overline{w's'}/u_*$; and that M-O length L is defined as
 230 (Hill 1989):

$$231 \quad L = u_*^2 \theta / [\kappa g (\theta_* + 0.61 \theta q_* / \rho_d)], \quad (12)$$

232 where ρ_d is the density of dry air.

233 A large number of research results show that, in the case of unstable stratification,
 234 $\phi_i(z/L)$ and $\phi_s(z/L)$ can be expressed in the following forms (Panofsky et al. 1977;
 235 Padro 1993; Katul et al. 1999):

$$236 \quad \phi_i(z/L) = c_1 (1 - c_2 z/L)^{1/3}; \quad (13)$$

$$237 \quad \phi_s(z/L) = \alpha_s (1 - \beta_s z/L)^{-1/3}. \quad (14)$$

238 where c_1 , c_2 , α and β are coefficients to be determined by the field observation. In the
 239 case of stable stratification, $\phi_s(z/L)$ is approximate to a constant and $\phi_i(z/L)$ is
 240 still the 1/3 function of z/L . The turbulent characteristics of the eddies in different
 241 temporal and spatial scales are analyzed and compared with the mean and
 242 autocorrelation ergodic theorems, to test the feasibility of MOS's relations under
 243 conditions of the ergodic and non-ergodic turbulence.

244 3 The sources and processing of data

245 In this study, the first turbulence data that were measured by the eddy correlation
 246 method under the homogeneous surface in the Nagqu Station of Plateau Climate and
 247 Environment (NSPCE), Chinese Academy of Sciences (CAS) are used. The data set in
 248 NSPCE/CAS includes that measured by 3-D sonic anemometer and thermometer

249 (CSAT3) with 10 Hz as well as infrared gas analyzer (Li7500) in ASL from 23 July
250 2011 to 13 September 2011. In addition, the second turbulence data set of CASES-99
251 (Poulos et al. 2002; Chang et al. 2002) is used to verify the ergodicity of turbulence
252 observed by multi-station. The data set includes ASL's data in seven observation
253 points. The sub-towers, sn1, sn2 and sn3 are located 100 m away from the central
254 tower, the sn4 is 280 m away, and tower sn5 and sn6 are located 300 m away. For
255 CASES-99, the data of sonic anemometer and thermometer (CSAT3) with 20 Hz and
256 the infrared gas analyzer (Li7500) at 10m on the central tower with 55 m height in
257 ASL. And other turbulence data include 3-D sonic anemometer (ATI) and Li7500 at
258 10 m height on six sub-towers surrounding the central tower. The two data sets for
259 completely different purposes are compared to test universality of the research results.

260 The geographic coordinate of NSPCE/CAS is 31.37°N, 91.90°E, and its altitude is
261 4509 m a.s.l. The observation station is built on flat and wide area except for a hill of
262 about 200 m at 2 km distance in the north, and floors area 8000m². The ground
263 surface is mainly composed of sandy soil mixed with sparse fine stones, and an alpine
264 meadow with vegetation of 10-20 cm. The roughness length and displacement height
265 of underlying surface of NSPCE's meadow is respectively determined to 0.009 m and
266 0.03 m by calculation. CASES-99 is located in prairie of Kansas US. The geographic
267 coordinate of CASES-99's central tower is 37.65°N, 96.74°W. The observation field
268 is flat and growth grasses about 20-50 cm during the observation period, while the
269 roughness length and the displacement height of the CASES-99's underlying surface
270 is 0.012 m and 0.06 m, respectively (Martano 2000).

271 The data are selected to study the ergodicity of the observed eddies. Firstly, the
272 inaccurate data in the measurements caused by spike are deleted before data analysis.
273 Subsequently, the data are divides into continuous sections of 5-hour, and the 1-hour
274 high frequency signals are obtained by applying filtering of Eqs. (8) and (9) on each
275 5-hour data. In order to delete further the abnormal inaccurate data, the 12 fragments
276 of 5-min variances of the velocity and temperature in 1-hour are calculated and
277 compared with each other. The data that the deviations are less than $\pm 15\%$ including
278 the instrumental error about $\pm 5\%$ are selected. Moreover, the ultrasonic temperature
279 pulsation signals are converted to absolute temperature pulsation signals (Schotanus et
280 al. 1983; Kaimal et al. 1991). Then all data without spike for 25 days are done the
281 coordinate rotation by using the plane fitting method to improve the installation level

282 of instrument (Wilczak 2001). The Webb correction (Webb et al. 1980) is the
283 component of surface energy balance in physical nature, but not the component of
284 turbulent eddy. However, this study is to analyze the ergodicity of turbulent eddies.
285 According to our preliminary analysis about the ergodicity of turbulent eddies, such
286 correlation may also cause the unreason deviation from the prediction shown in Eq.
287 (14). We thus do not perform Webb correction on our research objectives of the
288 ergodicity.

289 **4. Result analysis**

290 Applying the two sets of data from NSPCE and CASES-99, we have tested the
291 ergodicity of eddies in different temporal scales under the condition of steady
292 turbulence. Here, we carefully select the representative data measured at the level of
293 3.08m in NSPCE during three time frames, namely 3:00-4:00, 7:00-8:00 and
294 13:00-14:00 China Standard Time (CST) on 25 August in clear weather to test and
295 demonstrate the ergodicity of eddies in different temporal scales. These three time
296 frames can represent three situations, i.e. the nocturnal stable boundary layer, early
297 neutral boundary layer and midday convective boundary layer.

298 The trend correction (McMillen 1988; Moore 1986) is used to exclude the influence
299 of low-frequency trend effect. In order to acquire the effective information of eddies
300 in the different temporal scales, Eqs. (8) and (9) are used to perform band-pass
301 filtering of the turbulence data at 3.08 m in NSPCE, which is equivalent to the
302 correction of the high-pass filtering. In addition, the results of the time band-pass
303 filtering from $n=j$ to $n=N-j$ corresponding to Eqs. (8) and (9) acquire the information
304 of eddies in the corresponding temporal scale. The band-pass filtering information of
305 different time frames is thereby utilized to study the turbulence characteristics and
306 ergodicity of eddies in the different temporal scales of six time frames, including 2
307 min, 3 min, 5 min, 10 min, 30 min and 60 min.

308 **4.1 M-O eddy local stability and M-O stratification stability**

309 The M-O stratification stability z/L describe a whole characteristic between the
310 mechanical and buoyancy effects in ASL's turbulence, but this study will decompose
311 the turbulence into the different scale eddies. Considering that the features of different
312 scale eddies of the atmospheric turbulence varied with the atmospheric stability
313 parameter z/L , a M-O eddy local stability that is limited in the certain scale range of
314 eddies is defined as z/L_c , so as to analyze the relation between the stratification

315 stability and ergodicity of the wind velocity, temperature and other factors of the
316 different scale eddies. It is noted that the M-O eddy local stability, z/L_c , is different
317 from the M-O stratification stability, z/L .

318 As an example, the eddy local stability z/L_c in the different temporal scales of the
319 three time frames from nighttime to daytime is as shown in Table 1. The results show
320 that the eddy local stability z/L_c below 2 min in temporal scale during the nighttime
321 time frame of 3:00-4:00 is 0.59, thus it is stable stratification. But as the eddy
322 temporal scale gradually increases from 3 min, 5 min and 10 min to 60 min, the eddy
323 local stability, z/L_c , yet gradually decreases to 0.31 and 0.28. Even, beginning from 10
324 min in the temporal scale, the eddy local stability decreases from -0.01 to -0.07. It
325 seems that the eddy local stability gradually varies from stable to unstable as the eddy
326 temporal scale increases. During the morning time frame of 7:00-8:00, the eddy local
327 stability z/L_c from 2 min to 60 min in the temporal scale eventually decreases from
328 0.52, 0.38, 0.16 and 0.15 to -0.43 at 30 min and a minimum of -1.29 at 60 min. It
329 means that eddies in the temporal scales of 30 min and 60 min have high local
330 instability. However, during the midday time frame of 14:00-15:00, the eddies in the
331 temporal scales from 2 min to 60 min are unstable. Now $-z/L_c$ is defined as the eddy
332 local instability. As the eddy scale increases, the eddy local instability in the scales
333 from 2 min to 3 min also increases, and the instability value reaches the maximum of
334 0.44 when the eddy scale is 5 min; the eddy scale continuously increases, but the eddy
335 local instability decreases.

336 The M-O eddy local stability is not entirely the same as the M-O stratification
337 stability of ABL in the physical significance. The M-O stratification stability of ABL
338 indicates the overall effect of atmospheric stratification of the ABL on the stability
339 including all eddies in integral boundary layer. The M-O stratification stability z/L for
340 no filtering data to include the whole turbulent signals is stable 0.02 for 3:00-4:00
341 (CST), but unstable -0.004 and -0.54 for 7:00-8:00 and 13:00-14:00 (CST),
342 respectively. But the eddy local stability is only a local effect of atmospheric
343 stratification on the stability of eddies in a certain scale. As the eddy scale increases,
344 the eddy local stability z/L_c will vary accordingly. The aforesaid results indicate that
345 the local stability of small-scale eddies is stable in the nocturnal stable boundary layer,
346 but the nocturnal stable boundary layer is possibly unstable for the large-scale eddies,
347 so to result in a sink effect on the small-scale eddies, but a positive buoyancy effect on

348 the large-scale eddies. However, in the diurnal unstable boundary layer, the eddy local
349 instability of 3 min scale reaches the maximum. Then the instability gradually
350 decreases as the eddy scale increases. Therefore, eddies of 3 min scale hold maximum
351 buoyancy, but the eddy buoyancy decreases as the eddy scale increases. However, the
352 small-scale eddies are more stable than the large scale eddies in the nocturnal stable
353 boundary layer; while the large-scale eddies are more stable than the small scale
354 eddies in the diurnal unstable and convective boundary layers. The above facts signify
355 that it is common that there exist mainly the small-scale eddies in the nocturnal
356 boundary layer with stable stratification. And it is also common that there exist mainly
357 the large-scale eddies in the diurnal convective boundary layer with unstable
358 stratification. Therefore, it can well understand that the small-scale eddies are
359 dominant in the nocturnal stable boundary layer, while the large-scale eddies are
360 dominant in the diurnal convective boundary layer.

361 **4.2 Verification of mean ergodic theorem of the eddies in different temporal scale**

362 In order to verify the mean ergodic theorem, we calculated the mean and
363 autocorrelation functions using Eq. (2) and Eq. (3), then calculated the variation of
364 mean ergodic function $Ero(A)$ using Eq. (5) of eddies in the different temporal scale
365 with relaxation time τ to be cut off with $\tau_i=n$. The mean ergodic functions, $Ero(A)$, of
366 vertical velocity, temperature and specific humidity of the different scale eddies are
367 calculated by using the data at level of 3.08 m for the three time frames of 3:00-4:00,
368 7:00-8:00 and 13:00-14:00 (CST) in NSPCE, as shown in Figs. 1-3 respectively. Since
369 the ergodic function varies within a large range, the ergodic functions are normalized
370 according to the characteristic quantity of relevant variables ($A_* = u_*, |\theta_*|, |q_*|$). That is
371 to say, the functions in all following figures are dimensionless ergodic functions,
372 $Ero(A)/A_*$.

373 The comprehensive analyses of the mean ergodicity characteristics of atmospheric
374 turbulence and the relevant causes:

375 4.2.1 Verifying mean ergodic theorem of different scale eddies

376 According to the mean ergodic theorem, Eq. (4), the mean ergodic function $Ero(A)/A_*$
377 will converge to 0 if the time approaches infinite. This is a theoretical result of the
378 stationary random processes. However, the practical mean ergodic function is
379 calculated under the condition of that relaxation time $\tau_i=n$ is cut off. If the mean
380 ergodic function $Ero(A)/A_*$ converges approximately to 0 in relaxation time $\tau_i=n$, it will

381 be considered that random variable A approximately satisfies the mean ergodic
382 theorem. The mean ergodic function deviates more from zero, the mean ergodicity
383 will be of poor quality. So as we can judge approximately whether or not the mean
384 ergodic theorem of different scale eddies holds. Figs. 1-3 clearly show that, regardless
385 of the vertical velocity, temperature or humidity, the $Ero(A)/A^*$ of eddies below 10
386 min in the temporal scale will swing around zero within a small range; thus we can
387 conclude that the mean ergodic function $Ero(A)/A^*$ of eddies below 10 min in the
388 temporal scale converges to zero to satisfy effectively the conditions of mean ergodic
389 theorem. For eddies of 30 min and 60 min, which are larger scale, the mean ergodic
390 function $Ero(A)/A^*$ will deviate further from zero. In particular, the mean ergodic
391 function $Ero(A)/A^*$ of eddies of 30 min and 60 min of the temperature or humidity
392 does not converge, and even diverges. The above results show that the mean ergodic
393 function of eddies of 30 min and 60 min cannot converge to zero or cannot satisfy the
394 conditions of mean ergodic theorem.

395 4.2.2 Comparison of the convergence of mean ergodic functions of vertical velocity, 396 temperature and humidity

397 As seen from Figs. 1-3, the dimensionless mean ergodic function of the vertical
398 velocity is compared with the respective function of the temperature and humidity, it
399 is 3-4 magnitudes less than those in the nocturnal stable boundary layer; 1-2
400 magnitudes less than those in the early neutral boundary layer; and around 2
401 magnitudes less than those in the midday convective boundary layer. For example,
402 during nighttime time frame of 3:00-4:00 (CST), the dimensionless mean ergodic
403 function of vertical velocity is 10^{-5} in magnitude, while the respective magnitudes of
404 function value of the temperature and humidity are 10^{-1} and 10^{-2} ; during morning time
405 frame of 7:00-8:00 (CAT), the magnitude of mean ergodic function of the vertical
406 velocity is 10^{-4} , while the respective magnitudes of function value of the temperature
407 and humidity are 10^{-2} and 10^{-3} ; during midday time frame of 13:00-14:00 (CST), the
408 magnitude of mean ergodic function of the vertical velocity is 10^{-4} , while the
409 magnitudes of function value of the temperature and humidity are both 10^{-2} . These
410 results show that the dimensionless mean ergodic function of vertical velocity
411 converges to zero much more easily than respective function value of the temperature
412 and humidity, and that the vertical velocity satisfies the conditions of mean ergodic
413 theorem to overmatch the temperature and humidity.

414 4.2.3 Temporal scale and spatial scale of turbulent eddy

415 For wind velocity of $1-2 \text{ ms}^{-1}$, the eddy spatial scale in the temporal scale 2 min is
416 around 120-240 m, and the eddy spatial scale in the temporal scale 10 min is around
417 600-1200 m. The eddy spatial scale in the temporal scale 2 min is equivalent to the
418 ASL's height, and the eddy spatial scale in the temporal scale 10 min is equivalent to
419 ABL's height. The eddy spatial scale within the temporal scale 30-60 min is around
420 1800-3600 m, and this spatial scale clearly exceeds ABL's height to belong to the
421 scope of atmospheric local circulation. According to the stationary random processes
422 definition (1) and the mean ergodic theorem, the stationary random processes must be
423 smooth in the relaxation time τ . The eddies below temporal scale 10 min, i.e. below
424 ABL's height are the stationary random processes, and can effectively satisfy the
425 conditions of mean ergodic theorem. However, the eddies in the temporal scale 30
426 min and 60 min exceed the ABL's height do not satisfy the conditions of mean ergodic
427 theorem, thus these eddies belong to the non-stationary random processes.

428 4.2.4 Ergodicity of the turbulence of all eddies of possible scale in ABL

429 To facilitate comparison, Fig. 4 shows the variation of mean ergodic function $Ero(A)$
430 of the vertical velocity (a), temperature (b) and specific humidity (c) before filtering
431 with relaxation time τ during midday 14:00-15:00 (CST) in the convective boundary
432 layer. It is obvious that Fig. 4 is unfiltered mean ergodic function of eddies in all
433 possible scale in ABL. The Fig. 4 compares with Figs. 1c, 2c and 3c, which are the
434 mean ergodic function $Ero(A)/A^*$ of vertical velocity, temperature and humidity after
435 filtering during the midday time frame of 14:00-15:00 (CST). The result shows that
436 the mean ergodic functions before filtering are greater than that after filtering. As
437 shown in Figs. 1c, 2c and 3c, the magnitude for the vertical velocity is 10^{-4} and the
438 magnitudes for the temperature and specific humidity are both 10^{-2} . According to Fig.
439 4, the magnitude of vertical velocity $Ero(A)/A^*$ is 10^{-3} and the magnitudes of
440 temperature and specific humidity are both 10^0 , therefore 1-2 magnitudes are almost
441 decreased after filtering. Moreover, all trend upward for vertical velocity and
442 temperature and downward for specific humidity, deviating from zero. It is thus clear
443 that, even if the midday 14:00-15:00 (CST). when is equivalent to local time
444 12:00-13:00, the mean ergodic function of eddies in all possible scale in the
445 convective boundary layer cannot converge to zero before filtering, i.e. cannot satisfy
446 the conditions of mean ergodic theorem. That may be that eddies in all possible scale

447 before filtering including the local circulation in convective boundary layer. So we
448 argue that, under general situations, the eddies only below 10 min in the temporal
449 scale or within 600-1200 m in the spatial scale in ABL are the ergodic stationary
450 random processes, but the turbulence including the eddies with all possible scale in
451 ABL may belong to the non-ergodic stationary random processes.

452 4.2.5 Relation between the ergodicity and local stability of different scale eddies

453 The corresponding eddy local stability z/L_c of eddies at different times in different
454 scales (see Table 1) show that the eddy local stability z/L_c of the different scale eddies
455 are different, due to the fact that the temperature stratification in ABL has different
456 effects on the stability of different scale eddies. Even entirely contrary results can
457 occur. At the same time the stratification which can cause the large scale eddy to
458 ascend with buoyancy may cause the small scale eddy to descend. However, the
459 analysis results in Figs. 1-3 show that the ergodicity is mainly related to the eddy
460 scale, and its relation with the atmospheric temperature stratification seems
461 unimportance.

462 **4.3 Verification of autocorrelation ergodic theorem for different scale eddies**

463 In this section, Eqs. (7a) and (7b) are used to verify the autocorrelation ergodic
464 theorem. It is identified in Sect. 4.2 that the turbulent eddies below 10 min in the
465 temporal scale satisfy the mean ergodic conditions in the various time frames, i.e. the
466 turbulent eddies below 10 min in the temporal scale are at least in strictly stationary
467 random processes or narrow stationary random processes in the nocturnal stable
468 boundary layer, early neutral boundary layer and midday convective boundary layer.
469 Then we analyze further the different scale eddies which satisfy the mean ergodic
470 conditions whether or not also satisfy the autocorrelation ergodic conditions, so as to
471 verify whether atmospheric turbulence is in the narrow or wide stationary random
472 processes. The autocorrelation ergodic function of turbulence variable A under the
473 condition of truncated relaxation time $\tau_{i=n}$ are calculated according to Eq. (7a) to
474 determine the variation of autocorrelation ergodic function $Er(A)$ with relaxation time
475 τ . As with the mean ergodic function $Ero(A)$, if the autocorrelation ergodic function
476 $Er(A)$ of the eddies of 2 min, 3 min, 5 min, 10 min, 30 min and 60 min in the temporal
477 scale within the relaxation time $\tau_{i=n}$ is approximate to 0, then A shall be deemed to be
478 approximately ergodic; the more the autocorrelation ergodic function deviates from 0,
479 the worse the autocorrelation ergodicity becomes. Therefore, this method can be used

480 to judge approximatively whether the different scale eddies satisfy the conditions of
481 autocorrelation ergodic theorem.

482 For example, Fig. 5 shows the variation of normalized autocorrelation ergodic
483 function $Ero(w)/u^*$ of the turbulent eddies of 2 min, 3 min, 5 min, 10 min, 30 min and
484 60 min in the temporal scale with relaxation time τ for the vertical velocity during the
485 time frames of 3:00-4:00, 7:00-8:00 and 13:00-14:00 (CST). Some basic conclusions
486 are drawn from Fig. 5:

- 487 1. After comparing Figs. 5a-c with Figs. 1a-c, i.e. comparing the dimensionless mean
488 ergodic function $Ero(w)/u^*$ of vertical velocity with the dimensionless
489 autocorrelation ergodic function $Er(w)/u^*$, two basic characteristics are very clear.
490 First, the magnitudes of the dimensionless autocorrelation ergodic function
491 $Er(w)/u^*$, regardless of whether in the nocturnal stable boundary layer, early neutral
492 boundary layer or midday convective boundary layer, are all greatly reduced. In
493 Figs. 1a-c, the magnitudes of $Ero(w)/u^*$ are respectively 10^{-5} , 10^{-4} and 10^{-4} , and the
494 magnitudes of $Er(w)/u^*$ are respectively 10^{-7} , 10^{-5} and 10^{-5} , as shown in Figs. 5a-c.
495 The magnitudes of $Er(w)/u^*$ reduce by 1-2 magnitudes compared with those of
496 $Ero(w)/u^*$. Second, all autocorrelation ergodic functions $Er(w)/u^*$ of the eddies of
497 30 min and 60 min in temporal scale, regardless of whether they are in the stable
498 boundary layer, natural boundary layer or convective boundary layer, are all
499 reduced and approximate to $Ero(w)/u^*$ of the eddies below 10 min in temporal
500 scale.
- 501 2. The above two basic characteristics imply that the autocorrelation ergodic function
502 $Er(w)/u^*$ of the stable boundary layer, neutral boundary layer or convective
503 boundary layer converges to 0 faster than the mean ergodic function $Ero(w)/u^*$; the
504 autocorrelation ergodic function of eddies of 30 min and 60 min in temporal scale
505 also converges to 0 and satisfies the conditions of autocorrelation ergodic theorem,
506 except for the fact that the autocorrelation ergodic function $Er(w)/u^*$ of the eddies
507 below 10 min in temporal scale can converge to 0 and satisfy the conditions of
508 autocorrelation ergodic theorem.
- 509 3. According to the autocorrelation ergodic function Eq. (7a), the eddies of 30 min, 60
510 min and below 10 min in the temporal scale, regardless of whether they are in the
511 stable boundary layer, neutral boundary layer or convective boundary layer, all
512 eddies can satisfy the conditions of autocorrelation ergodic theorem. Therefore, in

513 general the ABL's turbulence is the stationary random processes of autocorrelation
514 ergodicity.

515 4. The above results show that the eddies below 10 min in temporal scale in the
516 nocturnal stable boundary layer, early neutral boundary layer and midday
517 convective boundary layer can not only satisfy the conditions of mean ergodic
518 theorem, but also they can also satisfy the conditions of autocorrelation ergodic
519 theorem. Therefore, the eddies below 10 min in the temporal scale are wide ergodic
520 stationary random processes. Although the eddies of 30 min and 60 min in
521 temporal scale in the stable boundary layer, neutral boundary layer and convective
522 boundary layer can satisfy the conditions of autocorrelation ergodic theorem, but
523 they cannot satisfy the conditions of mean ergodic theorem. Therefore, eddies of 30
524 min and 60 min in the temporal scale are neither narrow ergodic stationary random
525 processes, nor wide ergodic stationary random processes.

526 **4.4 Ergodic theorem verification of different scale eddies for the multiple stations**

527 The basic principle of turbulence average is the ensemble average of the space, time
528 and state. Sections 4.2 and 4.3 verify the mean ergodic theorem and autocorrelation
529 ergodic theorem of atmospheric turbulence during the stationary random processes
530 using field observational data, so that the finite time average of a single station can be
531 used to substitute for the ensemble average. This section examines the ergodicity of
532 different scale eddies according to the observational data from the CASES-99's center
533 tower and six sub-sites (in all seven stations). When the data are selected, it is
534 considered that if the eddies are not evenly distributed at the seven stations, then the
535 observation results at the seven stations may have originated from many eddies in the
536 large scale. For this reason, we first compared the high frequency variance spectrum
537 above 0.1 Hz. Based on the observational error, if the difference of all high frequency
538 variances does not exceed the average by $\pm 10\%$, then it is assumed that the turbulence
539 is evenly distributed at the seven observation stations. Finally, 17 datasets are chosen
540 from among the turbulence observation data from 5 to 30 October, and these data sets
541 refer to the results of strong turbulence at noon on a sunny day. As an example, the
542 same method as described in Sections 4.2 and 4.3 is used to respectively calculate the
543 variation of the mean ergodic function and the autocorrelation ergodic function of
544 vertical velocity in 10:00-11:00 on 7 October with relaxation time τ . Next, the
545 observation data chosen from the seven stations are built into a data set, and the time

546 series of data set are filtered at 2 min, 3 min, 5 min, 10 min, 30 min and 60 min. The
547 variations of mean ergodic function $Ero(w)/u^*$ and autocorrelation ergodic function
548 $Er(w)/u^*$ of the vertical velocity with relaxation time τ are analyzed to test the
549 ergodicity of different scale eddies for the observation of multi-station. Fig. 6a shows
550 the variation of mean ergodic function $Ero(w)/u^*$ of the vertical velocity with the
551 relaxation time τ , and Fig. 6b shows the variation of autocorrelation ergodic function
552 $Er(w)/u^*$ with the relaxation time τ .

553 The results show ergodic characteristics of different scale eddies measured at the
554 multi-stations as following:

555 Fig. 6a shows that the mean ergodic function of eddies below 30 min in temporal
556 scale converges to 0 very well, except for the fact that the mean ergodic function of
557 eddies of 60 min in temporal scale clearly deviates upward from 0. Fig. 6b shows that
558 all autocorrelation ergodic functions of different scale eddy, including eddies of 60
559 min in temporal scale, gradually converge to 0. Therefore, eddies below 30 min in
560 temporal scale measured at the multi-stations satisfy the conditions of both the mean
561 and autocorrelation ergodic theorems, while eddies of 60 min in temporal scale only
562 satisfies the conditions of autocorrelation ergodic theorem, but cannot satisfy the
563 conditions of mean ergodic theorem. These facts demonstrate that eddies below 30
564 min in temporal scale are wide ergodic stationary random processes in the data series
565 composed by the seven stations. This signifies that the comparing of data series
566 composed of multiple stations with data from a single station, the eddy temporal scale
567 for wide ergodic stationary random processes is extended from below 10 min to 30
568 min. As analyzed above, if the eddies below 10 min in temporal scale are deemed to
569 be the turbulent eddies in the ABL with height about 1000 m and the eddies of 30 min
570 in the temporal scale, which is equivalent to that the space scale is greater than 2000
571 m, are deemed including the eddy components of local circulation in ABL, then
572 multiple station observations can completely capture the local circulated eddies,
573 which space scale is greater than 2000 m.

574 **4.5 Average time problem of turbulent quantity averaging**

575 The atmospheric observations are impossible to repeat experiment exactly, must use
576 the ergodic hypothesis and replace ensemble averages with time averages. It arises a
577 problem how does determine the averaging time.

578 The analyses on the ergodicity of different scale eddies in above two sections

579 demonstrate that the eddies below 10 min in temporal scale as $\tau=30$ min in the stable
580 boundary layer, neutral boundary layer and convective boundary layer can not only
581 satisfy the conditions of mean ergodic theorem, but also can also satisfy the
582 conditions of autocorrelation ergodic theorem. That is to say, they are namely wide
583 ergodic stationary random processes. Therefore, the finite time average of 30 min
584 within relaxation time τ can be used for substituting for the ensemble average to
585 calculate mean random variable Eq. (2). However, the eddies of 30 min and 60 min in
586 the temporal scale in the stable boundary layer and neutral boundary layer are only
587 autocorrelation ergodic random processes, neither narrow nor wide sense random
588 processes. Therefore, when the finite time average of 30 min can be used for
589 substituting for the ensemble average to calculate mean random variable Eq. (2), it
590 may capture the eddies below 10 min in temporal scale in stationary random processes,
591 but not completely capture the eddies above 30 min in the temporal scale. The above
592 results signify that the turbulence average is restricted not only by the mean ergodic
593 theorem, but also is closely related to the scale of turbulent eddy. In the observation
594 performed using the eddy correlation method, the substitution of ensemble average
595 with finite time average of 30 min inevitably results in a high level of error, due to
596 lack of low frequency component information of the large-scale eddies. However,
597 although eddies of 30 min and 60 min in the temporal scale in convective boundary
598 layer are not wide ergodic stationary random processes, they are autocorrelation
599 ergodic random processes. This may imply that the mean random variable which is
600 calculated with the finite time average in the convective boundary layer to substitute
601 for the ensemble average is often superior to the results of the stable boundary layer
602 and neutral boundary layer. Withal, the results in the previous sections also show that
603 the mean ergodic function of vertical velocity may more easily converge to 0 than
604 functions corresponding to the temperature and humidity, and the vertical velocity
605 may more easily satisfy the conditions of mean ergodic theorem than the temperature
606 and humidity. Therefore, in the observation performed using the eddy correlation
607 method, the result of vertical velocity is often superior to those of the temperature and
608 humidity. In this section, the results also point out that multi-station observation can
609 completely capture the local circumfluence eddies in the ABL. Therefore, the ergodic
610 assumption is more likely to be satisfied, and its results are much closer to the true
611 values when calculating the turbulence mean, variance or fluxes with the multi-station

612 observation data.

613 In order to determine the averaging time, Oncley (1996) defined an Ogive function
614 of cumulative integral

$$615 \quad Og_{x,y}(f_0) = \int_{\infty}^{f_0} Co_{x,y}(f) df \quad (15)$$

616 where x and y are any two variables whose covariance is \overline{xy} , $Co_{xy}(f)$ is the
617 cospectrum of xy . If the Ogive function converges to a constant value at a frequency
618 $f=f_0$, which could be converted to the averaging time of the measurement. The Ogive

619 of $\overline{u'w'}$ is often examined to determine the least averaging time. As a comparison,

620 here the variation of Ogive functions of $\overline{w'^2}$ and $\overline{u'w'}$ with frequency at the height
621 3.08 m in NSPCE for the three time frames is shown in Fig.7. Fig.7 shows the

622 variation of Ogive convergence frequency for $\overline{w'^2}$ in the nighttime stable conditions,
623 morningtide neutral boundary layer and midday convection boundary layer converges
624 respectively converges about 0.01 Hz, 0.0001 Hz and 0.001 Hz. It is equivalent to the

625 averaging times about 2 min, 160 min and 16 min. However for $\overline{u'w'}$, it converges
626 about 0.001 Hz only in the midday convection boundary layer to be equivalent to the
627 averaging time about 16 min. However it seems no convergence in the nighttime

628 stable and morningtide neutral boundary layer. It is implied determining averaging
629 time seems to have a bit difficult with the Ogive function in the stable and neutral
630 boundary layer. The Fig.7 shows also that when the frequency is lower than 0.0001Hz,

631 Ogive functions $\overline{u'w'}$ ascend in the stable boundary layer, and descend in the
632 morningtide neutral boundary layer and midday convection boundary layer. It may be

633 low frequency effect caused the cross local circulation in the nighttime and midday in
634 ABL. Especially we must note that the Ogive is a function of the cumulative integral.

635 So as Ogive changes direction from ascending to descending, it implies that in the
636 negative momentum flux superimposing positive flux. The foremost reason that there

637 exists the positive up momentum flux at 3m level in the ASL is a local circulation
638 effect highly possible. The local circulation in ABL may be a cause that Ogive fails to

639 judge the averaging time. In this work, the choice of averaging time with the ergodic
640 theory seems superior to with the Ogive function.

641 **4.6 MOS of turbulent eddies in different scales and its relation with ergodicity**

642 Turbulent variance is a most basic characteristic quantity of the turbulence.

643 Turbulence velocity variance, which represents turbulence intensity, and the variance
 644 of scalars, such as temperature and humidity, effectively describes the structural
 645 characteristics of turbulence. In order to test MOS relation of the different scale
 646 eddies with ergodicity, the vertical velocity and temperature data of NSPCE from 23
 647 July to 13 September are used to determine the MOS relationship of variances of
 648 vertical velocity and temperature for the different scale eddies, and analyze its relation
 649 with the ergodicity.

650 The MOS relation of vertical velocity variance as following:

$$651 \quad \phi_i(z/L) = c_1(1 - c_2 z/L)^{1/3}, \quad z/L < 0, \quad (16)$$

$$652 \quad \phi_i(z/L) = c_1(1 + c_2 z/L)^{1/3}, \quad z/L > 0. \quad (17)$$

653 Fig. 8 and 9 respectively shows the MOS relation curves of different scale eddies for
 654 the vertical velocity and temperature variances in NSPCE. The figures (a), (b) and (c)
 655 of Fig. 8 and 9 are respectively the similarity curve of eddies of 10 min, 30 min and
 656 60 min in the temporal scale. Table 2 shows the relevant parameters of fitting curve of
 657 MOS relation for the vertical velocity variance. The correlation coefficient and
 658 residual of fitting curve are respectively expressed with R and S .

659 Fig. 8 and Table 2 show that the parameters of fitting curve are greatly different,
 660 even if the fitting curve modality of MOS relation of the vertical velocity variance for
 661 the eddies in different temporal scales is the same. The correlation coefficients of
 662 MOS's fitting curve of the vertical velocity variance under the unstable stratification
 663 are large, but the correlation coefficients under the stable stratification are small.
 664 Under unstable stratification, the correlation coefficient of eddies of 10 min in the
 665 temporal scale reaches 0.97, while the residual is only 0.16; under the stable
 666 stratification, the correlation coefficient reduces to 0.76, and the residual increases to
 667 0.25. With the increase of eddy temporal scale from 10 min (Fig. 8a) to 30 min (Fig.
 668 8b) and 60 min (Fig. 8c), the correlation coefficients of MOS relation of the vertical
 669 velocity variance gradually reduce, and the residuals increase. The correlation
 670 coefficient in 60 min is the minimum; it is only 0.83 under the unstable stratification,
 671 and only 0.30 under the stable stratification.

672 The temperature variance is shown in Fig. 9. The MOS's function to fit from eddies
 673 of 10 min in the temporal scale under the unstable stratification is following:

$$674 \quad \phi_\theta(z/L_c) = 4.9(1 - 79.7 z/L_c)^{-1/3}. \quad (18)$$

675 As shown in Fig. 9a, the correlation coefficient of fitting curve is -0.91 and residual is
676 0.38. With the increase of eddy temporal scale, discreteness of MOS relation of the
677 temperature variance is enlarged quickly, and an appropriate curve cannot be fitted.

678 The above results show that the discreteness of fitting curve of MOS relation for
679 the turbulence variance is enlarged with the increase of eddy temporal scale for either
680 the vertical velocity or temperature. The points of data during the stationary processes
681 basically gather nearby the fitting curve of variance similarity relation, while all data
682 points during the nonstationary processes deviate significantly from the fitting curve.
683 However, the similarity of vertical velocity variance is superior to that of the
684 temperature variance. These results are consistent to the conclusions of testing
685 ergodicity for the different scale eddies described in Sections 4.2-4.4. The ergodicity
686 of small-scale eddy is superior to that of the larger-scale eddy, and eddies of 10 min in
687 the temporal scale has the best variance similarity function. These results also signify
688 that when the eddy at the stationary random processes satisfies the ergodic conditions,
689 then both the vertical velocity variance and temperature variance of eddies in the
690 different temporal scales comply with MOST very well; but, as for eddies with poor
691 ergodicity during nonstationary random processes, the variances deviate from MOS
692 relations.

693 **5 Conclusion**

694 From the above results, we can draw the below preliminary conclusions:

- 695 1. The turbulence in ABL is an eddy structure. When the temporal scale of turbulent
696 eddies in ABL is about 2 min, the corresponding spatial scale is about 120-240 m
697 to be equivalent to ASL's height; when the temporal scale of turbulent eddies in
698 ABL is about 10 min, the corresponding spatial scale is about 600-1200 m to be
699 equivalent to the ABL's height. For the eddies in larger temporal and spatial scale,
700 such as eddies of 30-60 min in the temporal scale, the corresponding spatial scale
701 is about 1800-3600 m. Spatial scale exceeds the ABL's height.
- 702 2. For the atmospheric turbulent eddies below the ABL's scale, i.e. the eddies below
703 1000 m in the spatial scale and 10 min in the temporal scale, the mean ergodic
704 function $Ero(A)$ and autocorrelation ergodic function $Er(A)$ converge to 0, i.e. they
705 can satisfy the conditions of mean and autocorrelation ergodic theorem. However,
706 for the atmospheric turbulent eddies above 2000-3000m in the spatial scale and
707 above 30-60 min in the temporal scale, the mean ergodic function doesn't converge

708 to 0, thus cannot satisfy the conditions of mean ergodic theorem. Therefore, the
709 turbulent eddies below the ABL's scale belong to the wide ergodic stationary
710 random processes, but the turbulent eddies which are larger than ABL's scale
711 belong to the non-ergodic random processes, or even the nonstationary random
712 processes.

713 3. Due to above facts, when the stationary random process information of eddies
714 below 10 min in the temporal scale and below 1000 m of ABL's height in the
715 spatial scale can be captured, the atmospheric turbulence may satisfy the conditions
716 of mean ergodic theorem. Therefore, an average of finite time can be used for
717 substituting for the ensemble average of infinite time to calculate mean random
718 variable as measuring atmospheric turbulence with the eddy correlation method.
719 But for the turbulence of eddies above 30 min in temporal scale and above 2000 m
720 in spatial scale magnitude, it cannot satisfy the conditions of mean ergodic theorem,
721 so that the eddy correlation method cannot completely capture the information of
722 nonstationary random processes. This will inevitably cause a high level of error
723 due to the lack of low frequency component information of the large-scale eddies
724 when the average of finite time is used to substitute for the ensemble average in
725 observation.

726 4. Although the atmospheric temperature stratification has different effects on the
727 stability of eddies in the different scales, the ergodicity is mainly related to the
728 local stability of eddies, and its relation with the stratification stability of ABL is
729 not significant.

730 5. The data series composed from seven stations compare with the observational data
731 from a single station. The results show that the temporal and spatial scale of eddies
732 to belong to the wide ergodic stationary random processes are extended from 10
733 min to below 30 min and from 1000 m to below 2000 m respectively. This signifies
734 that the ergodic assumption is more likely to be satisfied well with multi-station
735 observation data, and observational results produced by the eddy correlation
736 method are much closer to the true values when calculating the turbulence average,
737 variance or fluxes.

738 6. If the ergodic conditions of stationary random processes are more effectively
739 satisfied, then the turbulence variance of eddies in the different temporal scales
740 can comply with MOST very well; however, the turbulence variance of the

741 non-ergodic random processes deviates from MOS relations.

742

743 **6 Discussion**

744 1. Galanti (2004) proved that the turbulence which was temporally steady and
745 spatially homogeneous is ergodic, but ‘partially turbulent flows’ such as the mixed
746 layer, wake flow, jet flow, flow around and boundary layer flow may be
747 non-ergodic turbulence. However, it has been proven through atmospheric
748 observational data that the turbulence ergodicity is related to the scale of turbulent
749 eddies. Since the large-scale eddies in ABL may be strongly influenced by the
750 boundary disturbance, thus belong to ‘partial turbulence’; however, since the
751 small-scale eddies in atmospheric turbulence may be not influenced by boundary
752 disturbance, may be temporally steady and spatially homogeneous turbulence. So
753 that the mean ergodic theorem and autocorrelation ergodic theorem for the
754 turbulent eddies in small scale in ABL is applicative, but the large-scale eddies are
755 non-ergodic.

756 2. The eddy correlation method for turbulence measurement is based on the ergodic
757 assumption. A lack of ergodicity related to the presence of large-scale eddy
758 transport can lead to a consider error of the flux measurement. This has already
759 been pointed out by Mauder et al. (2007) or Foken et al. (2011). Therefore, we
760 realize from the above conclusions that the large scale eddies may include
761 non-ergodic random process components which exceed ABL’s height. The eddy
762 correlation method for the measurement and calculation of turbulent variance and
763 covariance can not capture the information of large-scale eddy exceeded ABL’s
764 scale, thus resulting in large error. MOST is developed on the conditions of steady
765 time and homogeneous surface. MOST’s conditions, steady time and homogeneous
766 surface, are in line with the ergodic conditions, therefore the turbulence variance,
767 even the turbulent fluxes of eddies in the different temporal scales may comply
768 with MOST very well, if the ergodic conditions of stationary random processes are
769 more effectively satisfied.

770 3. According to Kaimal and Wyngaard (1990), the atmospheric turbulence theory and
771 observation method were feasible and led to success under ideal conditions
772 including a short period, steady state and homogeneous underlying surface, and
773 through observation in the 1950s-1970s, but these conditions are rare in reality. In
774 the land surface processes and ecosystem, the turbulent flux observation in ASL is

775 a scientific issue in which commonly interest researchers in the fields of
776 atmospheric science, ecology, geography science, etc. These observations must be
777 implemented under conditions such as with complex terrain, heterogeneous surface,
778 long period and unsteady state. It is necessary that more neoteric observational
779 tools and theories will be applied with new perspectives in future research.

780 4. It is successful that the banausic ergodic theorem of stationary random processes is
781 introduced from the mathematics into atmospheric sciences. It undoubtedly
782 provides a profited tool for overcoming the challenges which encounter during the
783 modern measurement of atmospheric turbulent flow. At least it offers a promising
784 first step to diagnosticate directly the ergodic hypotheses for ASL's flows as a
785 criterion. And that the necessary and sufficient conditions of ergodic theorem can
786 introduce to the applicative scope of eddy correlation method and MOST, and seek
787 potential reasons disable for using them in the ABL.

788 5. In the future, we shall keep up to study the ergodic problems for the atmospheric
789 turbulence measurement under the conditions of complex terrain, heterogeneous
790 surface and unsteady, long observational period, and to seek effective schemes. The
791 above results indicate the atmospheric turbulent eddies below the scale of ABL can
792 be captured by the eddy correlation method and comply with MOST very well.
793 Perhaps MOST can be as the first order approximation to deal with the turbulence
794 of eddies below ABL's scale satisfying the ergodic theorems, then to compensate
795 the effects of eddies dissatisfying the ergodic theorems, which may be caused by
796 the advection, local circulation, low frequency effect, etc under the complex terrain,
797 heterogeneous surface. For example, we developed a turbulent theory of
798 non-equilibrium thermodynamics (Hu, Y., 2007; Hu, Y., et al., 2009) to find the
799 coupling effects of vertical velocity, which is caused by the advection, local
800 circulation, and low frequency, on the vertical fluxes. The coupling effects of
801 vertical velocity may be as a scheme to compensate the effects of eddies
802 dissatisfying the ergodic theorems (Hu, Y., 2003; Chen, J., et al., 2007, 2013).

803 6. It is clear that such studies are preliminary, and many problems require further
804 research. The attestation of more field experiments is necessary.

805

806 *Acknowledgements.* This study is supported by the National Natural Science
807 Foundation of China under Granted Nos. 91025011, 91437103 and National Program

808 on Key Basic Research Project (2010CB951701-2). This work was strongly supported
809 by the Heihe Upstream Watershed Ecology-Hydrology Experimental Research Station,
810 Chinese Academy of Sciences. I would like to express my sincere regards for their
811 support, and also thank Dr. Gordon Maclean of NCAR for providing the detailed
812 CASES-99 data used in this study. We thank referees very much for heartfelt
813 comments, discussion and marked errors.

814

815 References

816 Aubinet, M., Vesala, T., and Papale, D.: Eddy covariance, a practical guide to
817 measurement and data analysis, Springer, Dordrecht, Heidelberg, London, New
818 York, 438, 2012.

819 Birkhoff, G. D.: Proof of the ergodic theorem, Proc. Nat. Acad. Sci. USA. 18,
820 656-660, 1931.

821 Boltzmann, L.: Analytischer beweis des zweiten Hauptsatzes der mechanischen
822 Wärmetheorie aus den Sätzen über das Gleichgewicht der lebendigen Kraft, Wiener
823 Berichte , 63, 712-732, in WAI, paper 20, 1871.

824 Chang, S. S. and Huynh, G. D.: Analysis of sonic anemometer data from the
825 CASES-99 field experiment. Army Research Laboratory, Adelphi, MD. 2002.

826 Chen, J., Hu Y., and Zhang L.: Principle of cross coupling between vertical heat
827 turbulent transport and vertical velocity and determination of cross coupling
828 coefficient, Adv. Atmos. Sci., 23 (4), 639-648, 2007.

829 Chen, J., Hu, Y., Lu, S., and Yu, Ye.: Experimental demonstration of the coupling
830 effect of vertical velocity on latent heat flux, Sci. China. Ser. D-Earth Sci., 56,
831 1-9, 2013.

832 Eichinger, W. E., Parlange, M. B., Katul, G. G.: Lidar measurements of the
833 dimensionless humidity gradient in the unstable ASL, Lakshmi, V., Albertson, J.
834 and Schaake, J., Koster, R. D., Duan, Q., Land Surface Hydrology, Meteorology,

835 and Climate, American Geophysical Union, Washington, D. C. 7-13, 2001.

836 Foken, T., Wichura, B.: Tools for quality assessment of surface-based flux
837 measurements. *Agric For Meteorol.*, 78, 83-105, 1996.

838 Foken, T., Göckede, M., Mauder, M., Mahrt, L., Amiro, B. D., and Munger, J. W.:
839 Post-field data quality control, in: *Handbook of micrometeorology: a guide for*
840 *surface flux measurement and analysis*, Lee, X., Massman, W. J., and Law, B.:
841 Kluwer, Dordrecht, 181-208, 2004.

842 Foken, T., Aubinet, M., Finnigan, J. J., Leclerc, M. Y., Mauder, M., Paw, U. K. T.:
843 Results of a panel discussion about the energy balance closure correction for
844 trace gases. *Bull Am. Meteorol. Soc.*, 92(4), ES13-ES18, 2011.

845 Galanti, B. and Tsinober, A.: Is turbulence ergodic? *Physics Letters A*, 330, 173–18,
846 2004.

847 Higgins, C. W., Katul, G. G., Froidevaux, M., Simeonov, V. and Parlange, M. B.:
848 Atmospheric surface layer flows ergodic? *Geophys. Res. Lett.*, 40, 3342-3346,
849 2013.

850 Hill, R. J.: Implications of Monin–Obukhov similarity theory for scalar quantities, *J.*
851 *Atmos. Sci.* 46, 2236–2244, 1989.

852 Hu, Y.: Convergence movement influence on the turbulent transportation in
853 atmospheric boundary layer, *Adv. Atmos. Sci.*, **20**(5), 794-798, 2003.

854 Hu, Y., Chen, J., Zuo, H.: Theorem of turbulent intensity and macroscopic mechanism
855 of the turbulence development, *Sci China Ser D-Earth Sci*, **37**(2), 789-800, 2007.

856 Hu, Y., and Chen, J.: Nonequilibrium Thermodynamic Theory of Atmospheric
857 Turbulence, In: *Atmospheric Turbulence, Meteorological Modeling and*
858 *Aerodynamics*, Edited by Peter R. Lang and Frank S., Nova Science Publishers,
859 Inc., 59-110, 2009.

860 Kaimal, J. C. and Wyngaard, J. C.: The Kansas and Minnesota experiments, Bound.
861 Lay. Meteor., 50, 31-47, 1990.

862 Kaimal, J. C. and Gaynor, J. E.: Another look at sonic thermometry, Bound. Lay.
863 Meteor., 56, 401-410, 1991.

864 Katul, G. G., Hsieh, C. I.: A note on the flux-variance similarity relationships for heat
865 and water vapor in the unstable atmospheric surface layer, Bound. Lay. Meteor., 90,
866 327-338, 1999.

867 Katul, G., Cava, D., Poggi, D., Albertson, J., and Mahrt, L.: Stationarity, homogeneity,
868 and ergodicity in canopy turbulence, Handbook of micrometeorology a guide for
869 surface flux measurement and analysis, Lee, X., Kluwer Academic Publishers,
870 New York, 161-180, 2004.

871 Krenkel, U.: Ergodic theorems, de Gruyter, Berlin, New York, 363, 1985.

872 Lennaert van, V., Shigeo, K., and Genta, K.: Periodic motion representing isotropic
873 turbulence, Fluid Dyn. Res., 38, 19-46, 2006.

874 Li, X., Hu, F., Pu, Y., Al-Jiboori, M. H., Hu, Z., and Hong, Z.: Identification of
875 coherent structures of turbulence at the atmospheric surface layer, Adv. Atmos.
876 Sci., 19(4), 687-698, 2002.

877 Mauder, M., Desjardins, R. L., MacPherson, J.: Scale analysis of airborne flux
878 measurements over heterogeneous terrain in a boreal ecosystem. J. Geophys. Res.
879 112, D13112, 2007.

880 Martano, P.: Estimation of surface roughness length and displacement height from
881 single-level sonic anemometer data, J. Appl. Meteorol., 39(5), 708-715, 2000.

882 Mattingly, J. C.: On recent progress for the stochastic Navier Stokes equations,
883 Journées équations aux dérivées partielles, Univ. Nantes, Nantes, Exp. No. XI,
884 1-52, 2003.

885 McMillen, R. T.: An eddy correlation technique with extended applicability to non
886 simple terrain, *Bound. Lay. Meteor.*, 43, 231-245, 1988.

887 Moore, C. J.: Frequency response corrections for eddy correlation systems, *Bound.*
888 *Lay. Meteor.*, 37, 17-35, 1986.

889 Neumann, J. V.: Proof of the quasi-ergodic hypothesis, *Mathematics Proc. N. A. S.*,
890 18, 70-82, 1932.

891 Oncley, S. P., Friehe, C. A., John, C. L., Businger, J. A., Itsweire, E. C., Chang, S. S.:
892 Surface-Layer Fluxes, Profiles, and Turbulence Measurements over Uniform
893 Terrain under Near-Neutral Conditions, *J. Atmos. Sci.*, 53 (7), 1029-1044, 1996.

894 Padro, J.: An investigation of flux-variance methods and universal functions applied
895 to three land-use types in unstable conditions, *Bound. Lay. Meteor.*, 66, 413-425,
896 1993.

897 Panofsky, H. A., Lenschow, D. H., and Wyngaard, J. C.: The characteristics of
898 turbulent velocity components in the surface layer under unstable conditions. *Bound.*
899 *Lay. Meteor.*, 11, 355-361, 1977.

900 Papoulis, A. and Pillai, S. U.: *Probability, random variables and stochastic processes.*
901 McGraw-Hill. New York. 666, 1991.

902 Poulos, G. S., Blumen, W., Fritts, D. C., Lundquist, J. K., Sun, J., Burns, S. P., Nappo,
903 C., Banta, R., Newsom, R., Cuxart, J., Terradellas, E., and Balsley, Ben.: CASES-99:
904 a comprehensive investigation of the stable nocturnal boundary layer. *Bull. Amer.*
905 *Meteor. Soc.*, 83, 555-581, 2002.

906 Schotanus, P., Nieuwstadt, F. T. M., and de Bruin, H. A. R.: Temperature measurement
907 with a sonic anemometer and its application to heat and moisture fluxes, *Bound.*
908 *Lay. Meteor.*, 26, 81-93, 1983.

909 Stull, R. B.: *An introduction to boundary layer meteorology.* Kluwer Academic Publ.

910 Dordrecht. 670, 1988.

911 Uffink, J.: Boltzmann'S work in statistical physics, Stanford encyclopedia of
912 philosophy, Edward, N. Z., 2004.

913 Vickers, D., Mahrt, L.: Quality control and flux sampling problems for tower and
914 aircraft data. J. Atmos. Oceanic. Technol., 14, 512-526, 1997.

915 Webb, E. K., Pearman, G. I., and Leuning, R.: Correction of the flux measurements for
916 density effects due to heat and water vapor transfer, Q. J. R. Meteorol. Soc., 106,
917 85–100, 1980.

918 Wilczak, J. M., Oncley, S. P., Stage, S. A.: Sonic anemometer tilts correction
919 algorithms. Bound. Lay. Meteor., 99(1), 127-150, 2001.

920 Wyngaard, J. C.: Turbulence in the atmosphere, getting to know turbulence,
921 Cambridge University Press, 2010.

922 Zuo, H., Xiao X., Yang Q., Dong L., Chen J., Wang S.: On the atmospheric movement
923 and the imbalance of observed and calculated energy in the surface layer, Sci. China.
924 Ser. D-Earth Sci., 55(9), 1518-1532, 2012.

925

926

927
928

Te 1 Local Stability Parameter $(z-d)/L_c$ of the Eddies in Different Temporal Scales on August 25

Time	3:00-4:00	7:00-8:00	14:00-15:00
Eddy scale			
≤ 2 min	0.59	0.52	-0.38
≤ 3 min	0.31	0.38	-0.44
≤ 5 min	0.28	0.16	-0.40
≤ 10 min	-0.01	0.15	-0.34
≤ 30 min	-0.04	-0.43	-0.27
≤ 60 min	-0.07	-1.29	-0.30

929

Te 2 Parameters of the Fitting Curve of MOS relation for Vertical Velocity Variance

	10 min		30 min		60 min	
	$z/L < 0$	$z/L > 0$	$z/L < 0$	$z/L > 0$	$z/L < 0$	$z/L > 0$
c_1	1.08	1.17	1.06	1.12	0.98	1.06
c_2	4.11	3.67	3.64	3.27	4.62	2.62
R	0.97	0.76	0.94	0.56	0.83	0.30
S	0.19	0.25	0.17	0.27	0.25	0.31

930

931

932

933

934

935

936

937

938

939

940

941

942

943

944

945

946

947

948

949

950

951

952

953

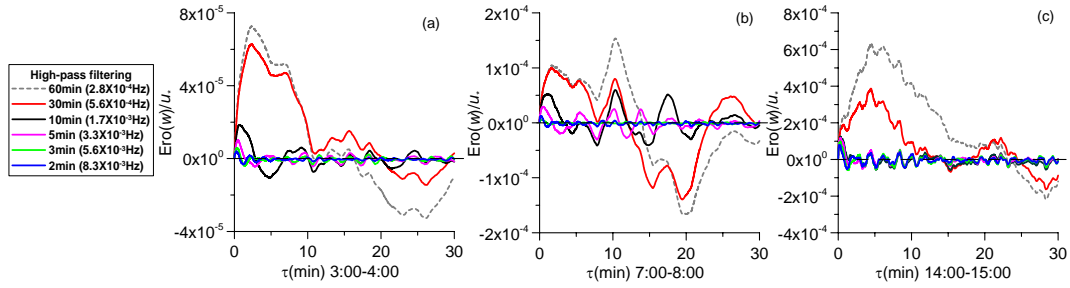


Fig. 1. Variation of mean ergodic function $Ero(w)$ of vertical velocity measured at the height 3.08 m in NSPCE with relaxation time for the different scale eddies after High-pass filtering. Panels (a), (b) and (c) are the respective results of the three time frames. If their mean ergodic function is more approximate to zero, then the average of eddies in the corresponding temporal scale will more closely satisfy the ergodic conditions.

956

957

958

959

960

961

962

963

964

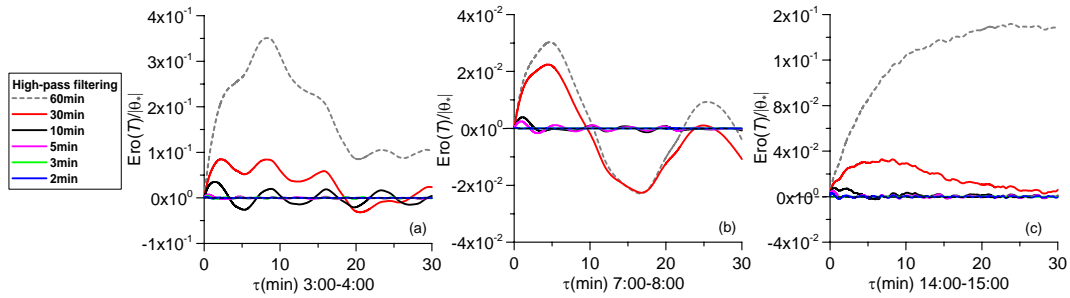


Fig. 2. Variation of mean ergodic function $Ero(T)$ of the different scale eddies of temperature with relaxation time (other conditions are similar to Fig. 2, and the same applies to the following figures).

967

968

969

970

971

972

973

974

975

976

977

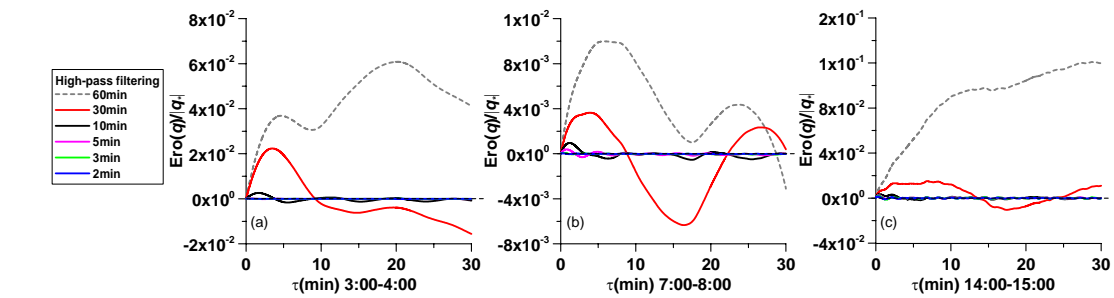


Fig. 3. Variation of mean ergodic function $Ero(q)$ of the different scale eddies of humidity with relaxation time.

978

979

980

981

982

983

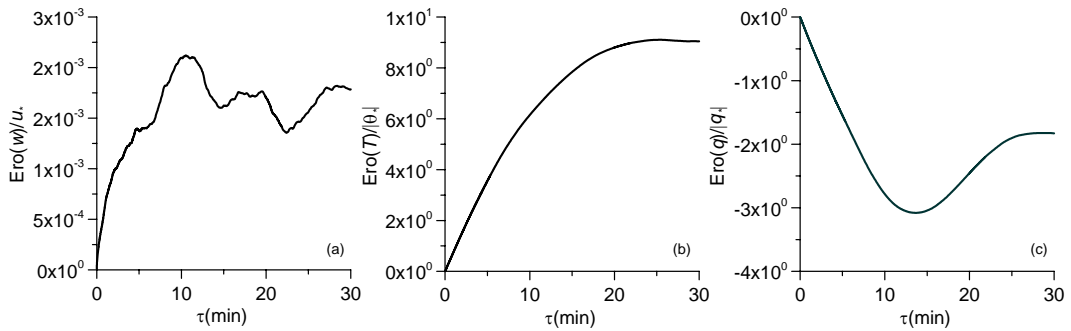
984

985

986

987

988



989 Fig. 4. Variation of mean ergodic function $Ero(w)$ of the vertical velocity (a), temperature (b) and specific humidity (c) before filtering during midday 14:00-15:00 (CST) in NSPCE with relaxation time τ .

990

991

992

993

994

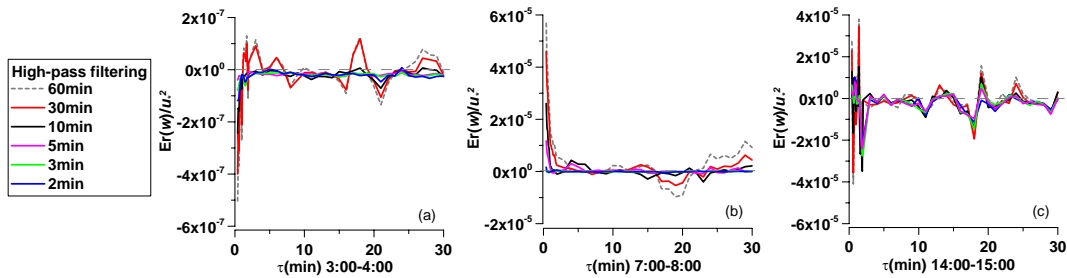
995

996

997

998

999



1000

1001 Fig. 5. Variation of the autocorrelation ergodic function of vertical velocity with relaxation time for different scale eddies.

1002

1003

1004

1005

1006

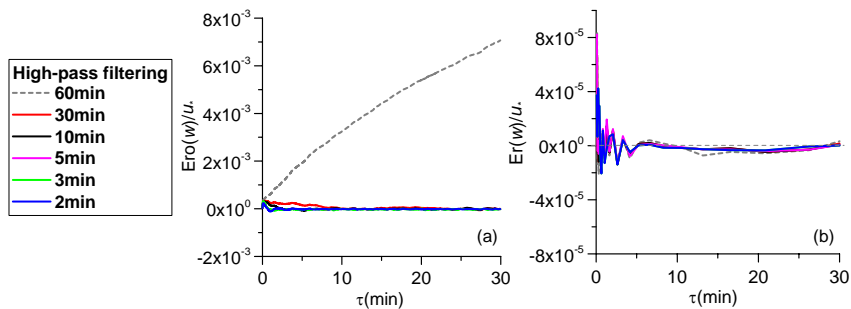
1007

1008

1009

1010

1011



1012 Fig. 6. Variation of mean ergodic function (a) and autocorrelation ergodic function (b) of the vertical velocity with relaxation time for the different scale eddies in CASES-99's seven stations.

1012
 1013
 1014
 1015
 1016

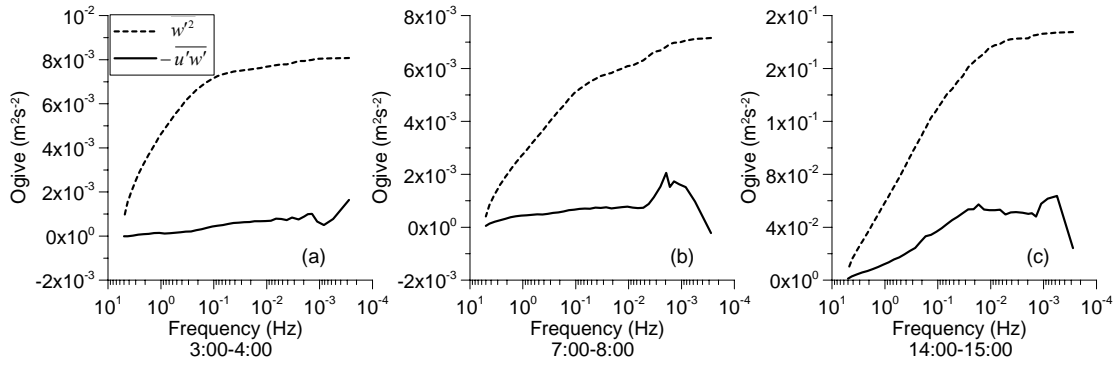


Fig. 7. Variation of Ogive functions of $\overline{w'^2}$ and $-\overline{u'w'}$ with frequency at the height 3.08 m in NSPCE for the three time frames.

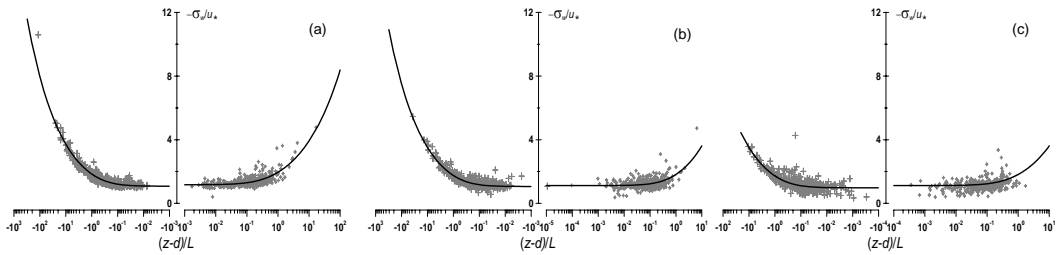


Figure 8. MOS relation of vertical velocity variances of the different scale eddies in NSPCE; Panels (a), (b) and (c) respectively represent the similarity of eddies of 10 min, 30 min and 60 min in the temporal scale.

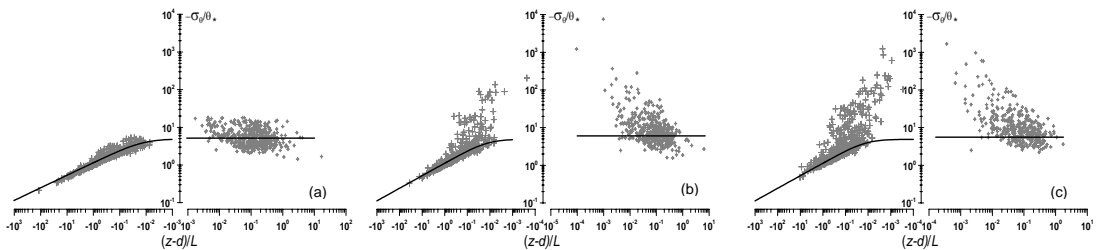


Figure 9. MOS relations of temperature variance of in different scale eddies of NSPCE; Panels (a), (b) and (c) respectively represent the similarity of the eddies of 10 min, 30 min and 60 min in the temporal scale.